

RESEARCH

Open Access



Detecting lesion-specific ischemia in patients with coronary artery disease with computed tomography fractional flow reserve measured at different sites

Zhaoxi Cai^{1†}, Taihui Yu^{1†}, Zehong Yang¹, Huijun Hu¹, Yongqing Lin², Haifeng Zhang², Meiwei Chen¹, Guangzi Shi¹ and Jun Shen^{1*}

Abstract

Objectives Whether a stenosis can cause hemodynamic lesion-specific ischemia is critical for the treatment decision in patients with coronary artery disease (CAD). Based on coronary computed tomography angiography (CCTA), CT fractional flow reserve (FFR_{CT}) can be used to assess lesion-specific ischemia. The selection of an appropriate site along the coronary artery tree is vital for measuring FFR_{CT}. However the optimal site to measure FFR_{CT} for a target stenosis remains to be adequately determined. The purpose of this study was to determine the optimal site to measure FFR_{CT} for a target lesion in detecting lesion-specific ischemia in CAD patients by evaluating the performance of FFR_{CT} measured at different sites distal to the target lesion in detecting lesion-specific ischemia with FFR measured with invasive coronary angiography (ICA) as reference standard.

Methods In this single-center retrospective cohort study, a total of 401 patients suspected of having CAD underwent invasive ICA and FFR between March 2017 and December 2021 were identified. 52 patients having both CCTA and invasive FFR within 90 days were enrolled. Patients with vessels 30%–90% diameter stenosis as determined by ICA were referred to invasive FFR evaluation, which was performed 2–3 cm distal to the stenosis under the condition of hyperemia. For each vessel with 30%–90% diameter stenosis, if only one stenosis was present, this stenosis was selected as the target lesion; if serial stenoses were present, the stenosis most distal to the vessel end was chosen as the target lesion. FFR_{CT} was measured at four sites: 1 cm, 2 cm, and 3 cm distal to the lower border of the target lesion (FFR_{CT}-1 cm, FFR_{CT}-2 cm, FFR_{CT}-3 cm), and the lowest FFR_{CT} at the distal vessel tip (FFR_{CT}-lowest). The normality of quantitative data was assessed using the Shapiro–Wilk test. Pearson's correlation analysis and Bland–Altman plots were used for assessing the correlation and difference between invasive FFR and FFR_{CT}. Correlation coefficients derived from Chi-square test were used to assess the correlation between invasive FFR and the combination of FFR_{CT} measured at four sites. The performances of significant obstruction stenosis (diameter stenosis ≥ 50%) at CCTA and FFR_{CT} measured at the four sites and their combinations in diagnosing lesion-specific ischemia were evaluated by receiver-operating characteristic (ROC) curves using invasive FFR as the reference standard. The areas under ROC curves (AUCs) of CCTA and FFR_{CT} were compared by the DeLong test.

[†]Zhaoxi Cai and Taihui Yu contributed equally to this work.

*Correspondence:

Jun Shen

shenjun@mail.sysu.edu.cn

Full list of author information is available at the end of the article



Results A total of 72 coronary arteries in 52 patients were included for analysis. Twenty-five vessels (34.7%) had lesion-specific ischemia detected by invasive FFR and 47 vessels (65.3%) had no lesion-specific ischemia. Good correlation was found between invasive FFR and FFR_{CT}-2 cm and FFR_{CT}-3 cm ($r=0.80$, 95% CI, 0.70 to 0.87, $p<0.001$; $r=0.82$, 95% CI, 0.72 to 0.88, $p<0.001$). Moderate correlation was found between invasive FFR and FFR_{CT}-1 cm and FFR_{CT}-lowest ($r=0.77$, 95% CI, 0.65 to 0.85, $p<0.001$; $r=0.78$, 95% CI, 0.67 to 0.86, $p<0.001$). FFR_{CT}-1 cm + FFR_{CT}-2 cm, FFR_{CT}-2 cm + FFR_{CT}-3 cm, FFR_{CT}-3 cm + FFR_{CT}-lowest, FFR_{CT}-1 cm + FFR_{CT}-2 cm + FFR_{CT}-3 cm, and FFR_{CT}-2 cm + FFR_{CT}-3 cm + FFR_{CT}-lowest were correlated with invasive FFR ($r=0.722$; 0.722; 0.701; 0.722; and 0.722, respectively; $p<0.001$ for all). Bland–Altman plots revealed a mild difference between invasive FFR and the four FFR_{CT} (invasive FFR vs. FFR_{CT}-1 cm, mean difference -0.0158, 95% limits of agreement: -0.1475 to 0.1159; invasive FFR vs. FFR_{CT}-2 cm, mean difference 0.0001, 95% limits of agreement: -0.1222 to 0.1220; invasive FFR vs. FFR_{CT}-3 cm, mean difference 0.0117, 95% limits of agreement: -0.1085 to 0.1318; and invasive FFR vs. FFR_{CT}-lowest, mean difference 0.0343, 95% limits of agreement: -0.1033 to 0.1720). AUCs of CCTA, FFR_{CT}-1 cm, FFR_{CT}-2 cm, FFR_{CT}-3 cm, and FFR_{CT}-lowest in detecting lesion-specific ischemia were 0.578, 0.768, 0.857, 0.856 and 0.770, respectively. All FFR_{CT} had a higher AUC than CCTA (all $p<0.05$), FFR_{CT}-2 cm achieved the highest AUC at 0.857. The AUCs of FFR_{CT}-2 cm and FFR_{CT}-3 cm were comparable ($p>0.05$). The AUCs were similar between FFR_{CT}-1 cm + FFR_{CT}-2 cm, FFR_{CT}-3 cm + FFR_{CT}-lowest and FFR_{CT}-2 cm alone (AUC = 0.857, 0.857, 0.857, respectively; $p>0.05$ for all). The AUCs of FFR_{CT}-2 cm + FFR_{CT}-3 cm, FFR_{CT}-1 cm + FFR_{CT}-2 cm + FFR_{CT}-3 cm, FFR_{CT}-2 cm + FFR_{CT}-3 cm + FFR_{CT}-lowest (0.871, 0.871, 0.872, respectively) were slightly higher than that of FFR_{CT}-2 cm alone (0.857), but without significant differences ($p>0.05$ for all).

Conclusions FFR_{CT} measured at 2 cm distal to the lower border of the target lesion is the optimal measurement site for identifying lesion-specific ischemia in patients with CAD.

Keywords Coronary artery disease, Computed tomography angiography, Fractional flow reserve

Introduction

Coronary computed tomography angiography (CCTA) has been widely accepted as a reliable noninvasive assessment modality for excluding the presence of coronary artery significant obstructive disease ($\geq 50\%$ luminal narrowing) in low-to-intermediate-risk populations with a high negative predictive value [1–3]. However, its diagnostic specificity for assessing obstructive coronary artery disease (CAD) is still suboptimal. For example, in severely calcified plaques, luminal stenosis is often overestimated owing to calcium blooming. More importantly, CCTA cannot provide hemodynamic information to determine whether a particular stenotic lesion is associated with hemodynamically significant ischemia i.e., lesion-specific ischemia [4]. While exercise treadmill testing and stress echocardiography can assess overall ischemic burden, they are limited in locating lesion-specific ischemia on a per-vessel basis [5]. Therefore, accurate and prompt assessment of lesion-specific ischemia is critical in the management of stable CAD to improve its clinical outcomes and benefits as myocardial blood flow can be improved by medical therapy or revascularization procedures such as percutaneous coronary intervention (PCI) or coronary artery bypass graft surgery (CABG) [6].

Fractional flow reserve (FFR) is the gold standard for the assessment of lesion-specific ischemia to guide revascularization in stable CAD patients [7]. Clinically, FFR is measured along with invasive coronary angiography

(ICA) by placing a pressure guidewire beyond a stenotic lesion and measuring the ratio of mean distal coronary pressure to mean aortic pressure ratio under conditions of adenosine infusion to the maximum hyperemia. At present, invasive FFR has become a cornerstone in determining lesion-specific ischemia and appropriate decision-making [8]. Whereas, invasive FFR requires additional expensive instruments, and clinical application of invasive FFR-informed treatment decision-making is relatively limited. Only 10% to 20% of revascularization procedures have incorporated invasive FFR results into the treatment decisions [9].

Recently, FFR can be noninvasively calculated from anatomical CCTA data based on computational fluid dynamics (CFD) [10]. This CT-based FFR (FFR_{CT}) does not need additional imaging and vasodilator administration. FFR_{CT}, the ratio of the maximum coronary blood flow through a stenotic artery to the blood flow assumed to be free of stenosis in that artery, has been validated to be useful in diagnosing and excluding lesion-specific ischemia [11–13]. Compared with invasive FFR, FFR_{CT} can provide FFR information almost at any site along the entire epicardial coronary artery tree [14]. Whereas the diagnostic accuracy of FFR_{CT} was previously determined by comparing a single measurement site corresponding to invasive FFR at a specific location within the coronary artery [11–13]. Inconsistent measurement sites between FFR_{CT} and invasive FFR can lead to inconclusive diagnostic results and confuse decision-making [15,

16]. Therefore, how to select an appropriate site along the coronary artery tree to measure FFR_{CT} is clinically relevant for the management of CAD. However, the optimal site to measure FFR_{CT} for a target lesion remains to be adequately determined.

In this single-center retrospective cohort study, CAD patients who had undergone both CCTA and invasive FFR were included. The diagnostic performances of FFR_{CT} measured at different sites at 1 cm, 2 cm, and 3 cm distal to the lower border of the target lesion of the artery (FFR_{CT-1} cm, FFR_{CT-2} cm, FFR_{CT-3} cm), and the lowest FFR_{CT} value at the distal vessel tip in which diameter larger than 1.5 mm ($FFR_{CT-lowest}$) were assessed and compared with invasive FFR as the reference standard. The purpose of this study was to determine the optimal site to measure FFR_{CT} for a target lesion in detecting lesion-specific ischemia in CAD patients.

Materials and methods

Patients

This retrospective study was approved by the ethics review board of Sun Yat-Sen Memorial Hospital at Sun Yat-Sen University (SYSEC-KY-KS-2022-054; Guangzhou, China), and the need to obtain informed consent was waived. A total of 401 patients suspected of having

CAD underwent invasive ICA and FFR between March 2017 and December 2021 were identified from the hospital database. Patients were included if they had undergone CCTA and subsequent invasive FFR within 90 days. The exclusion criteria were as follows: without CCTA examination ($n=323$), CCTA performed more than 90 days before invasive FFR ($n=14$), prior history of PCI ($n=7$), or imaging quality of CCTA ineligible for FFR_{CT} calculation ($n=5$). Finally, a total of 52 patients with 72 coronary vessels were included for analysis. The flowchart of the patient enrollment pathway is shown in Fig. 1. The demographics and baseline clinical characteristics of 52 patients are listed in Table 1.

ICA and invasive FFR measurement

All patients underwent conventional ICA and invasive FFR using standard techniques [17]. Each of the three main coronary vessels (anterior descending branch, circumflex branch and right coronary) was included in the analysis. All vessel segments were evaluated by two cardiologists (Y.L., with 20 years of experience of coronary intervention, and H.Z., with 15 years of experience of coronary intervention). Vessels with 30%-90% diameter stenosis as determined by ICA were referred to invasive FFR evaluation. For each vessel, if only one lesion having

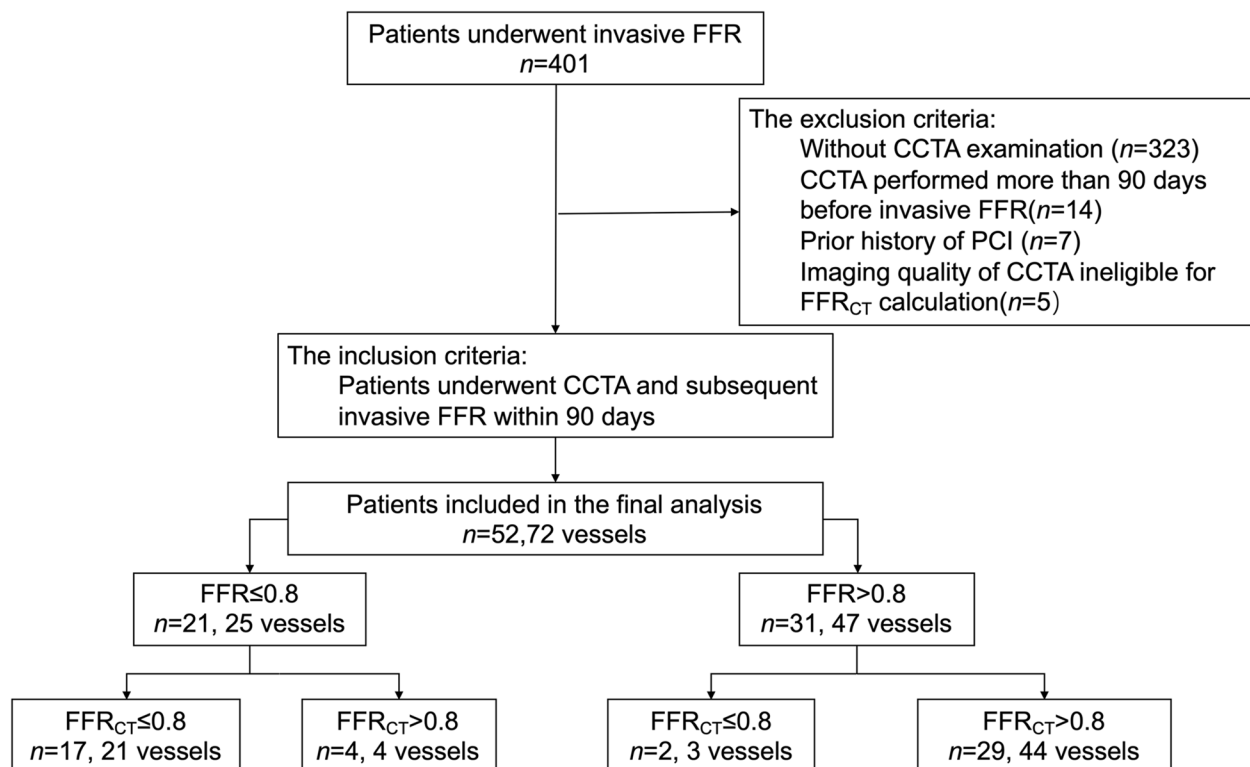


Fig. 1 Flowchart shows patient enrollment and exclusion. CCTA, coronary computed tomography angiography; PCI, percutaneous coronary intervention; FFR, fractional flow reserve; FFR_{CT} , computed tomography fractional flow reserve

Table 1 Demographics and baseline clinical characteristics of 52 patients with CAD

Characteristics	All Patients	Lesion-specific ischemia		p value
		Present	Absent	
No. of patients	52	21 (40.4)	31 (59.6)	
Age (years) ^a	66.7 ± 7.9	64.3 ± 8.6	68.5 ± 7.2	0.064
Gender				0.001
Male	25 (48.1)	16 (64.0)	9 (29.0)	
Female	27 (51.9)	5 (36.0)	22 (71.0)	
BMI(kg/m ²) ^a	24.8 ± 3.5	25.5 ± 3.7	24.3 ± 3.3	0.236
EF (%) ^a	69.4 ± 4.4	69.6 ± 4.6	69.3 ± 4.4	0.816
Risk factors				
Hypertension	31/52(59.6)	12/21 (57.1)	19/31 (61.3)	0.781
Diabetes mellitus	13/52(25.0)	5/21 (23.8)	8/31 (26.8)	1.000
Hyperlipidemia	22/52(42.3)	11/21 (52.4)	11/31 (35.5)	0.263
Smoking	13/52(25.0)	6/21 (28.6)	7/31 (22.6)	0.747
NYHA Classification				0.523
I	39/52(75.0)	17 (81.0)	22 (71.0)	
II	13/52(25.0)	4 (19.0)	9 (29.0)	
CAD in target vessels				
No. of vessels	72	25 (34.7)	47 (65.3)	
LAD	44 (61.1)	20 (45.5)	24 (54.5)	
LCX	12 (16.7)	3 (25.0)	9 (75.0)	
RCA	16 (22.2)	2 (12.5)	14 (87.5)	
CCTA (DS ≥ 50%)	63 (87.5)	25 (39.7)	38 (60.3)	
Interval between CCTA and invasive FFR (day) [†]	17.5(4.5–72)	11(5–39.5)	37(2–76)	0.815

Unless otherwise specified, data are numbers of patients, with percentages in parentheses. BMI body mass index, EF ejection fraction, NYHA New York Heart Association. CAD, coronary artery diseases, LAD left anterior descending artery, LCX left circumflex artery, RCA right coronary artery, CCTA coronary CT angiography, DS diameter stenosis

^a Data are means ± standard deviations. [†] Data are medians, with interquartile ranges in parentheses

30%–90% diameter stenosis was present, this lesion was selected as the target lesion according to the DeFACTO study [12]. If serial lesions were present, the lesion with 30%–90% diameter stenosis most distal to the vessel end was chosen as the target lesion according to the study by Nozaki et al. [18]. Lesion < 30% stenosis was not chosen as target lesion. For invasive FFR, a pressure-monitoring

guidewire (St Jude Medical, Minneapolis, Minn) was advanced 2–3 cm distal to the target lesion after administration of nitroglycerin [19]. Hyperemia was attained by intravenous administration of adenosine 5'-triphosphate at a dosage of 160 ug/kg/min. The lesion was considered lesion-specific ischemia when the measured FFR was ≤ 0.8.

CCTA protocol

CCTA was performed on a 64-slice CT scanner (SOMATOM Sensation 64; Siemens Healthineers, Forchheim, Germany or Discovery CT750HD; GE Healthcare, Pewaukee, WI, USA) with a retrospective ECG-gated technique or a third-generation 192-slice dual-source CT scanner (SOMATOM Force, Siemens Healthineers, Forchheim, Germany) with a prospective ECG-gated technique. The detailed CCTA protocols are listed in Table 2. Patient preparation and CT scanning were performed according to the Society of Cardiovascular Computed Tomography (SCCT) guidelines [20]. Patients with a heart rate > 70 beats/min were given oral beta-blockers (metoprolol tartrate tablets, 25–75 mg, AstraZeneca Pharmaceuticals China Co., LTD) 2 h before the CT scanning. In the absence of contraindications (hypotension, severe anemia, current use of nitrate medications, known nitroglycerin allergy), patients were given a 0.5 mg nitroglycerin tablet (Peking Yimin Pharmaceutical Co., Ltd) sublingually 2 min before scanning. CCTA images were obtained after intravenous injection of iodinated nonionic contrast agent (Iohexol; 350 mg/dl iodine, GE Healthcare, Cork, Ireland) at a dose of 1.0 ml/kg body weight with an infusion rate of 5 ml/s, followed by the injection of 40 ml saline at the same flow rate using a dual-head injector (Medrad stellant CT injector system; Medrad, Bayer Medical Care Inc, Indianola, PA, USA). Automatic bolus-tracking technology was used. The region of interest (ROI) was set at the ascending aorta of the aortopulmonary fenestration plane, and the triggering threshold value was 100 Hounsfield units. The scan range included the whole heart from the superior border of the aortic arch to the diaphragmatic surface of the heart. The CT technologists (H.H., with 20 years of experience in ECG-gated cardiac CT scanning) determined the optimal stationary cardiac phase images with

Table 2 Acquisition parameters of CCTA protocol

CT Scanners	Collimation	Rotation time	kVp	mAs	Slice thickness	Slice interval	Matrix	FOV
SOMATOM Force	96 × 0.6 mm	250 ms	70–100	320	0.6 mm	0.5 mm	512	211 mm
SOMATOM Sensation	64 × 0.6 mm	330 ms	120	900	0.6 mm	0.5 mm	512	211 mm
Discovery 750 HD	64 × 0.625 mm	330 ms	120	228	0.625 mm	0.625 mm	512	194 mm

FOV field of view

minimum motion-free and transferred them to an offline workstation for further analyses.

Morphologic analysis of CCTA

The CCTA images were analyzed by two radiologists with more than five years of experience (M.C., with 8 years of experience in cardiac imaging and G.S., with 7 years of experience in cardiac imaging) who were blinded to the ICA and invasive FFR results except for the location of the target lesion. The location of target lesion on CCTA was marked by the radiologist and the cardiologist together. The percentage diameter stenosis of the target lesion was measured using an offline quantitative coronary CT angiography software (Syngo-Via, Siemens Healthineers, Forchheim, Germany). Curved multiplanar reconstructions, maximum intensity projection (MIP), and volume rendering technique (VRT) were used to generate diagnostic images for interpretation. Lumen stenosis $\geq 50\%$ was defined as significant obstruction according to the SCCT guidelines [21].

FFR_{CT} analysis

FFR_{CT} analysis was performed using a dedicated software (RuiXin-FFR_{CT}, Raysight Inc., Shenzhen, Guangdong Province, China) which based on CFD to calculate FFR_{CT} using CCTA images. First, the initial segmentation model of the entire coronary artery was established, upon which the center line and contour of each coronary artery were obtained by the region growth algorithm. The contour was connected and smoothen to obtain a 3D model of the whole coronary artery. Then, the morphologic data of the heart were obtained according to CT images; Combined with the statistical prediction model of the basic characteristics of the patient (such as allometric growth law), the unique physiological indexes of the patient were obtained, such as the coronary artery pressure, coronary artery flow in the state of maximum congestion, microcirculation resistance, etc. Finally, an unstructured mesh was generated on the 3D model, and the blood was assumed to be a Newtonian liquid. The incompressible Navier Stokes equation was solved using the finite element algorithm to obtain the pressure and velocity of each grid point in the whole 3D coronary artery model, and then the FFR_{CT} value was obtained.

For each coronary artery, two radiologists (Z.Y., with fifteen years of experience in cardiac imaging; T.Y., with ten years of experience in cardiac imaging) who did not know the results of invasive FFR except for the location of target lesion independently measured FFR_{CT} at four sites as follows (Fig. 2), at 1 cm, 2 cm, 3 cm distal to the lower border of the target lesion of the artery (FFR_{CT}-1 cm, FFR_{CT}-2 cm, FFR_{CT}-3 cm), and the lowest FFR_{CT} value in the distal vessel tip (FFR_{CT}-lowest, coronary modeling

with FFR_{CT} data was limited to coronary vessels with a minimum luminal diameter of ≥ 1.5 mm), the position of FFR_{CT}-1 cm, FFR_{CT}-2 cm, FFR_{CT}-3 cm were measured on a reconstructed curved planar image. FFR_{CT} value of ≤ 0.80 was considered to be lesion-specific ischemia.

Statistical analysis

The normality of quantitative data was assessed using the Shapiro–Wilk test. Descriptive statistics were presented as mean \pm standard deviation (SD) for normally distributed variables. Non-normally distributed variables were expressed as the median and interquartile range (IQR), and categorical variables were expressed as numbers of cases (and percentages). Intraclass correlation coefficients (ICC) with a 95% confidence interval (CI) were used to assess the interobserver agreement in FFR_{CT}-1 cm, FFR_{CT}-2 cm, FFR_{CT}-3 cm and FFR_{CT}-lowest measurements. Data from two radiologists were averaged for analysis. Pearson's correlation analysis was used to evaluate the relationship between invasive FFR and FFR_{CT} values. Correlation coefficients derived from Chi-square test were used to assess the correlation between invasive FFR and the combination of FFR_{CT} measured at four sites. Bland–Altman plots were used to visualize the differences of invasive FFR and FFR_{CT} values. With invasive FFR as the reference standard, the accuracy, sensitivity, specificity, positive predictive value (PPV), and negative predictive value (NPV) of FFR_{CT}, the combination of FFR_{CT} measured at two or three sites, CCTA (significant obstruction stenosis, diameter stenosis $\geq 50\%$), and CCTA combined with each of FFR_{CT} measured at four sites in detecting lesion-specific ischemia were calculated. The performances of CCTA, FFR_{CT} measured at the four different sites and their combination in diagnosing lesion-specific ischemia were evaluated by receiver-operating characteristic (ROC) curves. The areas under the curve (AUCs) were compared using the DeLong method [22]. The sensitivities and specificities of FFR_{CT} and CCTA were compared by Chi-square, Fisher exact test, or McNemar test. Statistical analysis was performed using SPSS Statistics version 26 (IBM corporation, Armonk, NY, USA) or R 3.3.3 (R Foundation for Statistical Computing, Vienna, Austria) software. A *p* value < 0.05 was considered the significant threshold.

Results

Invasive FFR and FFR_{CT}

A total of 52 patients were included. Twenty-five vessels in 21 patients had lesion-specific ischemia as detected by invasive FFR. Forty-seven vessels in 31 patients had no lesion-specific ischemia as detected by invasive FFR. More male patients had lesion-specific ischemia (64.0% vs. 29.0%, *p* < 0.05) than female patients

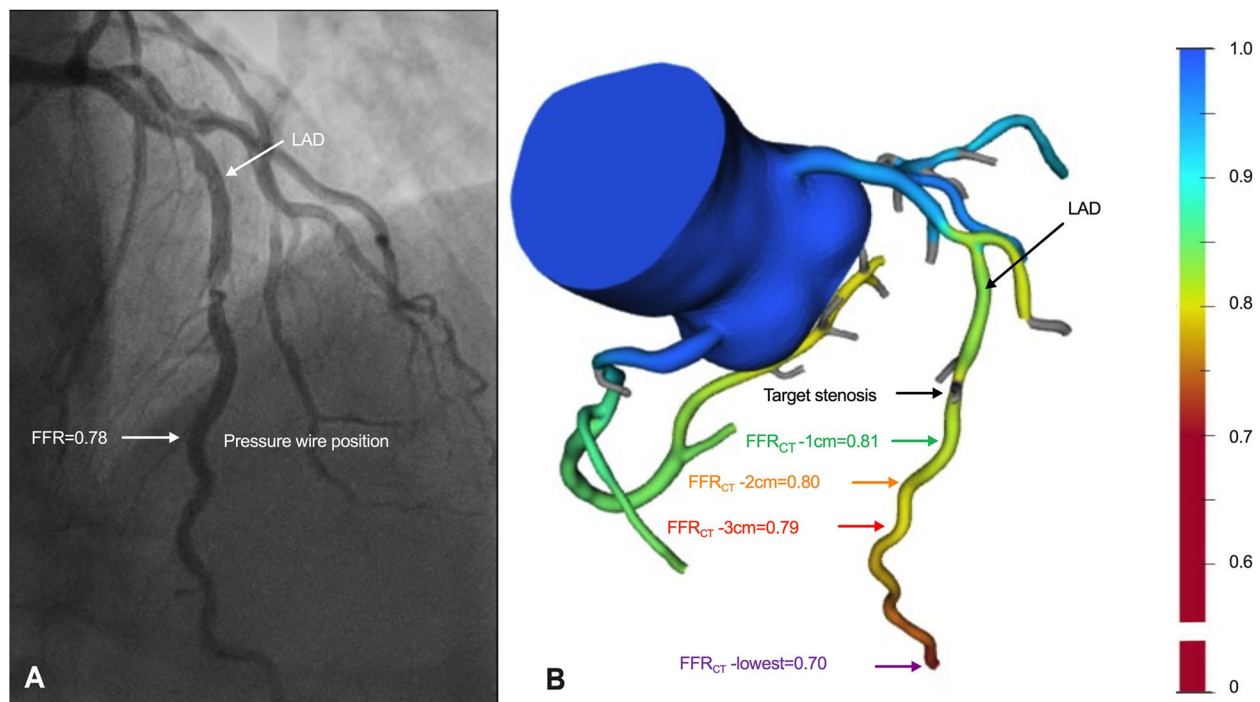


Fig. 2 Representative images for invasive FFR and FFR_{CT} measurements. **A** ICA image showing the tip of pressure-wire position in left anterior descending artery (LAD) during invasive FFR and the measured FFR was 0.78. **B** The corresponding pseudo-colored FFR_{CT} image show the site of target lesion and the measured FFR_{CT} at 1, 2, 3 cm distal to the target lesion (FFR_{CT}-1 cm, FFR_{CT}-2 cm, FFR_{CT}-3 cm) and the lowest FFR_{CT} (FFR_{CT}-lowest). LAD, left anterior descending artery; FFR, fractional flow reserve; FFR_{CT}, CT fractional flow reserve; FFR_{CT}-1 cm, FFR_{CT} measured at 1 cm distal to the lower border of the target lesion; FFR_{CT}-2 cm, FFR_{CT} measured at 2 cm distal to the lower border of the target lesion; FFR_{CT}-3 cm, FFR_{CT} measured at 3 cm distal to the lower border of the target lesion; FFR_{CT}-lowest, lowest FFR_{CT} value in the distal vessel tip

Table 3 Invasive FFR and FFR_{CT} of 72 vessels in 52 patients

Characteristics	All vessels	Lesion-specific ischemia		p value
		Present	Absent	
Invasive FFR	0.86 (0.77–0.93)	0.75 (0.67–0.78)	0.91 (0.86–0.95)	< 0.05
FFR _{CT} -1 cm	0.87 (0.80–0.92)	0.80 (0.77–0.84)	0.90 (0.86–0.94)	< 0.05
FFR _{CT} -2 cm	0.85 (0.79–0.91)	0.78 (0.82–0.80)	0.88 (0.84–0.93)	< 0.05
FFR _{CT} -3 cm	0.85 (0.78–0.90)	0.77 (0.70–0.79)	0.88 (0.83–0.92)	< 0.05
FFR _{CT} -lowest	0.80 (0.75–0.89)	0.73 (0.67–0.79)	0.86 (0.80–0.91)	< 0.05

Data are medians, with interquartile ranges in parentheses. FFR_{CT} CT fractional flow reserve, FFR fractional flow reserve

(Table 1). No significant differences were found in age, ejection fraction, New York Heart Association (NYHA) class, and body mass index (BMI) between patients with and without the lesion-specific ischemia ($p > 0.05$, Table 1). Invasive FFR and FFR_{CT} of 72 vessels in 52 patients with CAD are listed in Table 3. FFR_{CT}-1 cm, FFR_{CT}-2 cm, FFR_{CT}-3 cm, and FFR_{CT}-lowest in vessels

with lesion-specific ischemia were lower than those in vessels without lesion-specific ischemia ($p < 0.05$ for all).

Interobserver agreement

The ICCs in FFR_{CT} measurements between the two observers were 0.97 (95% CI, 0.96 to 0.98) for FFR_{CT}-1 cm, 0.98 (95% CI, 0.97 to 0.99) for FFR_{CT}-2 cm, 0.99 (95% CI, 0.98 to 0.99) for FFR_{CT}-3 cm, and 1.00 (95% CI, 0.99 to 1.00) for FFR_{CT}-lowest.

Correlation between FFR_{CT} and invasive FFR

Correlation analysis showed that there was a good correlation between invasive FFR and FFR_{CT}-2 cm ($r = 0.80$, 95% CI, 0.70 to 0.87, $p < 0.001$) and between invasive FFR and FFR_{CT}-3 cm ($r = 0.82$, 95% CI, 0.72 to 0.88, $p < 0.001$), there was a moderate correlation between invasive FFR and FFR_{CT}-1 cm ($r = 0.77$, 95% CI, 0.65 to 0.85, $p < 0.001$), and between invasive FFR and FFR_{CT}-lowest ($r = 0.78$, 95% CI, 0.67 to 0.86, $p < 0.001$) (Fig. 3A-D). Bland–Altman plots showed a mild difference between invasive FFR and FFR_{CT} on a per-vessel basis (invasive FFR vs. FFR_{CT}-1 cm, mean difference -0.0158, 95% limits of agreement: -0.1475 to 0.1159; invasive FFR vs. FFR_{CT}-2 cm, mean difference 0.0001, 95% limits of agreement: -0.1222 to 0.1220;

invasive FFR vs. $\text{FFR}_{\text{CT}-3}$ cm, mean difference 0.0117, 95% limits of agreement: -0.1085 to 0.1318; and invasive FFR vs. $\text{FFR}_{\text{CT}-\text{lowest}}$, mean difference 0.0343, 95% limits of agreement: -0.1033 to 0.1720) (Fig. 3E-H). Correlation analyses showed that $\text{FFR}_{\text{CT}-1}$ cm + $\text{FFR}_{\text{CT}-2}$ cm, $\text{FFR}_{\text{CT}-2}$ cm + $\text{FFR}_{\text{CT}-3}$ cm, $\text{FFR}_{\text{CT}-3}$ cm + $\text{FFR}_{\text{CT}-\text{lowest}}$, $\text{FFR}_{\text{CT}-1}$ cm + $\text{FFR}_{\text{CT}-2}$ cm + $\text{FFR}_{\text{CT}-3}$ cm, and $\text{FFR}_{\text{CT}-2}$ cm + $\text{FFR}_{\text{CT}-3}$ cm + $\text{FFR}_{\text{CT}-\text{lowest}}$ were correlated with invasive FFR ($r=0.722$; 0.722 ; 0.701 ; 0.722 ; and 0.722 , respectively; $p < 0.001$ for all).

Optimal measurement site of FFR_{CT}

ROC analyses of $\text{FFR}_{\text{CT}-1}$ cm, $\text{FFR}_{\text{CT}-2}$ cm, $\text{FFR}_{\text{CT}-3}$ cm, $\text{FFR}_{\text{CT}-\text{lowest}}$ per-vessel in identifying lesion-specific ischemia are shown in Table 4. The diagnostic sensitivity and NPV increased gradually with increasing of the distance from target lesion among the different measurement sites. $\text{FFR}_{\text{CT}-\text{lowest}}$ had lower accuracy and PPV than $\text{FFR}_{\text{CT}-2}$ cm, while had higher sensitivity than $\text{FFR}_{\text{CT}-2}$ cm (accuracy, $p=0.035$; sensitivity, $p=0.002$, and PPV, $p=0.037$, respectively). $\text{FFR}_{\text{CT}-\text{lowest}} \leq 0.8$ was found in 51.3% vessels (38/72) while $\text{FFR}_{\text{CT}-2} \leq 0.8$ was found in 33.3% (24/72) vessels. 18% vessels with $\text{FFR}_{\text{CT}-\text{lowest}} \leq 0.8$ were reclassified as negative according to their $\text{FFR}_{\text{CT}-2}$ cm values. There was no statistical significance in accuracy, sensitivity and NPV between $\text{FFR}_{\text{CT}-1}$ cm and $\text{FFR}_{\text{CT}-2}$ cm (accuracy, $p=0.123$; sensitivity, $p=0.977$, and NPV, $p=0.249$ respectively). The AUCs of $\text{FFR}_{\text{CT}-1}$ cm, $\text{FFR}_{\text{CT}-2}$ cm, $\text{FFR}_{\text{CT}-3}$ cm, $\text{FFR}_{\text{CT}-\text{lowest}}$ per-vessel in identifying lesion-specific ischemia using invasive FFR as reference standard were 0.768 (95% CI, 0.640 to 0.896), 0.857 (95% CI, 0.754 to 0.961), 0.856 (95% CI, 0.756 to 0.957) and 0.770 (95% CI, 0.657 to 0.882), respectively (Fig. 4), with the AUC of $\text{FFR}_{\text{CT}-2}$ cm being the greatest. The AUCs of $\text{FFR}_{\text{CT}-1}$ cm and $\text{FFR}_{\text{CT}-\text{lowest}}$ were significantly lower than that of $\text{FFR}_{\text{CT}-2}$ cm (0.770 vs. 0.857 for $\text{FFR}_{\text{CT}-\text{lowest}}$ vs. $\text{FFR}_{\text{CT}-2}$ cm, $p < 0.05$; 0.768 vs. 0.857 for $\text{FFR}_{\text{CT}-1}$ cm vs. $\text{FFR}_{\text{CT}-2}$ cm, $p < 0.05$). The AUCs showed no statistical significance between $\text{FFR}_{\text{CT}-2}$ cm and $\text{FFR}_{\text{CT}-3}$ cm ($p=0.295$).

The AUCs were similar between $\text{FFR}_{\text{CT}-1}$ cm + $\text{FFR}_{\text{CT}-2}$ cm (0.857 [95% CI, 0.754 to 0.961]), $\text{FFR}_{\text{CT}-3}$ cm + $\text{FFR}_{\text{CT}-\text{lowest}}$ (0.857 [95% CI, 0.756 to 0.957]) and $\text{FFR}_{\text{CT}-2}$ cm alone (0.857 [95% CI, 0.756 to 0.957]) ($p > 0.05$ for all). The AUCs of

$\text{FFR}_{\text{CT}-2}$ cm + $\text{FFR}_{\text{CT}-3}$ cm (0.871 [95% CI, 0.774 to 0.969]), $\text{FFR}_{\text{CT}-1}$ cm + $\text{FFR}_{\text{CT}-2}$ cm + $\text{FFR}_{\text{CT}-3}$ cm (0.871 [95% CI, 0.774 to 0.969]), and $\text{FFR}_{\text{CT}-\text{lowest}}$ + 2 cm + $\text{FFR}_{\text{CT}-3}$ cm + $\text{FFR}_{\text{CT}-\text{lowest}}$ (0.872 [95% CI, 0.774 to 0.970]) were slightly higher than that of $\text{FFR}_{\text{CT}-2}$ cm alone (0.857 [95% CI, 0.756 to 0.957]), but without significant differences ($p > 0.05$ for all).

Additive value of FFR_{CT}

The AUCs of CCTA ($\text{DS} \geq 50\%$) in identifying lesion-specific ischemia using invasive FFR as reference standard were 0.576 (95% CI, 0.443 to 0.713) (Table 4). The AUCs of FFR_{CT} measured at all the four different sites were significantly higher than CCTA DS (all $p < 0.05$). CCTA combined with any FFR_{CT} measured at 4 different sites had a higher AUC than CCTA alone (CCTA + $\text{FFR}_{\text{CT}-1}$ cm, 0.785 [95% CI, 0.664 to 0.905]; CCTA + $\text{FFR}_{\text{CT}-2}$ cm, 0.868 [95% CI, 0.770 to 0.967]; CCTA + $\text{FFR}_{\text{CT}-3}$ cm, 0.863 [95% CI, 0.765 to 0.961]; and CCTA + $\text{FFR}_{\text{CT}-\text{lowest}}$, 0.798 [95% CI, 0.695 to 0.902]; $p < 0.01$ for all).

Discussion

In this study, FFR_{CT} measured at four different sites along the coronary arteries was used to identify lesion-specific ischemia using invasive FFR as the reference standard. Our results showed that $\text{FFR}_{\text{CT}-2}$ cm had the highest accuracy (87.5%) and AUC (0.857) in identifying lesion-specific ischemia and $\text{FFR}_{\text{CT}-\text{lowest}}$ has the highest sensitivity and NPV than $\text{FFR}_{\text{CT}-1}$ cm, $\text{FFR}_{\text{CT}-2}$ cm, $\text{FFR}_{\text{CT}-3}$ cm. CCTA ($\text{DS} \geq 50\%$) combined with either $\text{FFR}_{\text{CT}-1}$ cm, $\text{FFR}_{\text{CT}-2}$ cm, $\text{FFR}_{\text{CT}-3}$ cm, or $\text{FFR}_{\text{CT}-\text{lowest}}$ showed higher AUC than CCTA alone in detecting lesion-specific ischemia.

Commonly, invasive FFR measurement is performed at one position selected 2-to-3 cm distal to the target lesion along coronary artery tree during ICA [19]. Unlike invasive FFR, FFR_{CT} values can be obtained along the entire coronary arterial tree. Inappropriate FFR_{CT} measurement can mislead the clinical decision. However, there is no consensus about the best location to measure FFR_{CT} in clinical practice. Previously, Cami et al. [16] used a CFD-based algorithm to measure FFR_{CT} value 10.5 mm (IQR 7.3–14.8 mm) distal to the stenosis in 26 patients with

(See figure on next page.)

Fig. 3 Scatter plots show a moderate correlation between invasive FFR and $\text{FFR}_{\text{CT}-1}$ cm (A) and between invasive FFR and $\text{FFR}_{\text{CT}-\text{lowest}}$ (B), a good correlation between invasive FFR and $\text{FFR}_{\text{CT}-2}$ cm (C) and between invasive FFR and $\text{FFR}_{\text{CT}-3}$ cm (D). Bland–Altman plots show a very mild difference between invasive FFR and $\text{FFR}_{\text{CT}-1}$ cm (E), invasive FFR and $\text{FFR}_{\text{CT}-2}$ cm (F), invasive FFR and $\text{FFR}_{\text{CT}-3}$ cm (G), invasive FFR and $\text{FFR}_{\text{CT}-\text{lowest}}$ (H) on a per-vessel basis. FFR, fractional flow reserve; FFR_{CT} , CT fractional flow reserve; $\text{FFR}_{\text{CT}-1}$ cm, FFR_{CT} measured at 1 cm distal to the lower border of the target lesion; $\text{FFR}_{\text{CT}-2}$ cm, FFR_{CT} measured at 2 cm distal to the lower border of the target lesion; $\text{FFR}_{\text{CT}-3}$ cm, FFR_{CT} measured at 3 cm distal to the lower border of the target lesion; $\text{FFR}_{\text{CT}-\text{lowest}}$, lowest FFR_{CT} value in the distal vessel tip

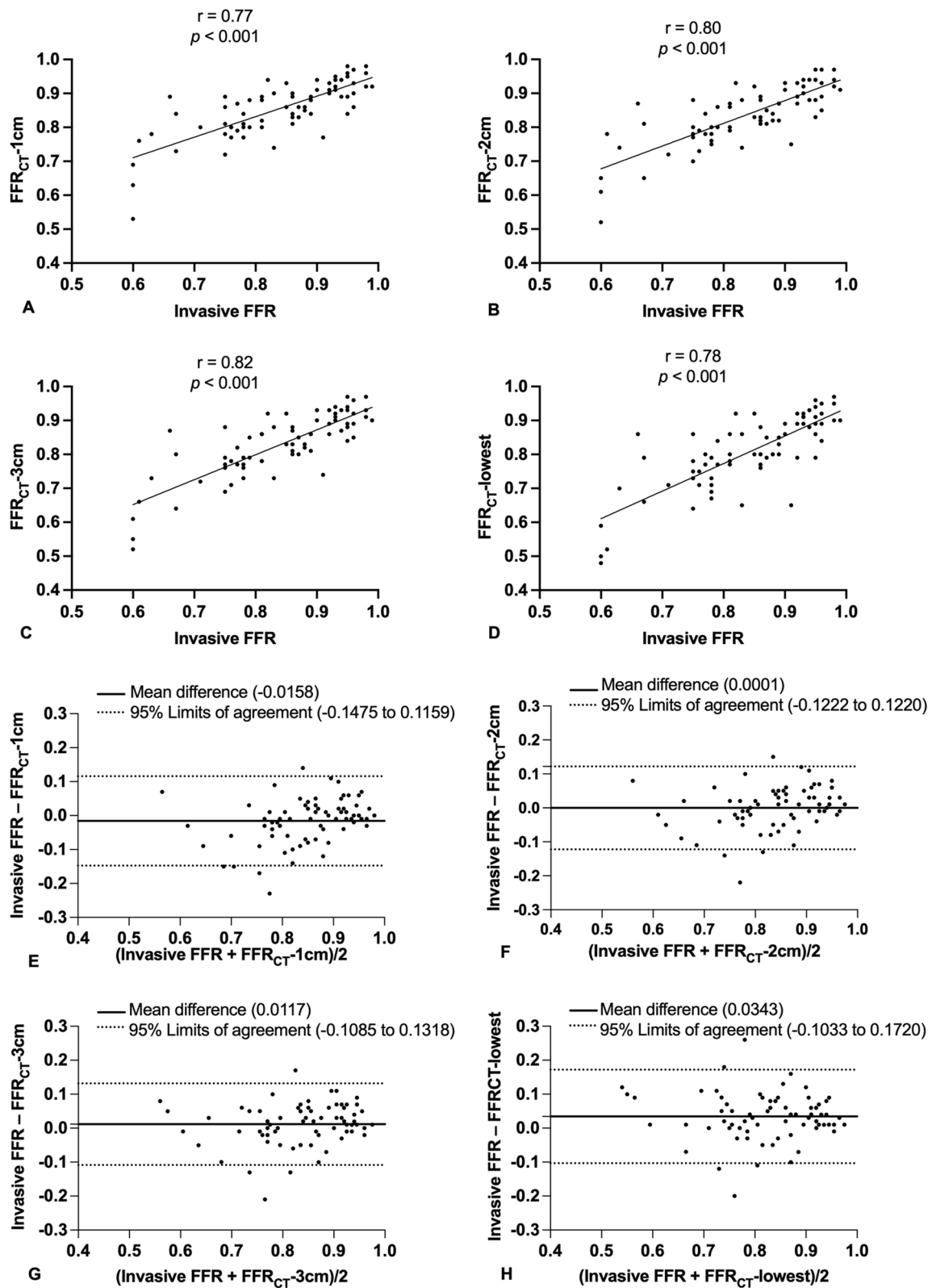


Fig. 3 (See legend on previous page.)

Table 4 ROC analysis of CCTA, FFR_{CT}-1 cm, FFR_{CT}-2 cm, FFR_{CT}-3 cm, FFR_{CT}-lowest and their combination in identifying lesion-specific ischemia on per-vessel basis

Per-vessel	Accuracy (%)	Sensitivity (%)	Specificity (%)	PPV (%)	NPV (%)	AUC	P value
CCTA (DS ≥ 50%)	47.2 (34/72) [36.1, 58.6]	100.0(25/25) [83.4, 100.0]	19.1(9/47) [9.6, 33.7]	39.7(25/63) [27.8, 52.8]	100.0 (9/9) [62.9, 100.0]	0.578 [0.443, 0.713]	0.277
FFR _{CT} -1 cm	81.9(59/72) [79.5, 89.1]	60.0(15/25) [38.9, 78.2]	93.6(44/47) [81.4, 98.3]	83.3(15/18) [57.7, 95.6]	81.5(44/54) [68.1, 90.3]	0.768 [0.640, 0.896]	0.0001
FFR _{CT} -2 cm	87.5(63/72) [77.9 93.3]	80.0(20/25) [58.7, 92.4]	91.5(43/47) [78.7, 97.2]	83.3(20/24) [61.8, 94.5]	89.6(43/48) [76.6, 96.1]	0.857 [0.754, 0.961]	0.0001
FFR _{CT} -3 cm	86.1(62/72) [76.3 92.3]	84.0(21/25) [63.1, 94.7]	87.2(41/47) [71.6, 93.5]	77.8(21/27) [54.8,88.6]	88.9(41/45) [77.9, 88.6]	0.856 [0.756, 0.957]	0.0001
FFR _{CT} -lowest	73.6(53/72) [62.4, 82.4]	88.0(22/25) [67.7, 96.8]	66.0(31/47) [50.6, 78.7]	58.0(22/38) [40.9, 73.3]	91.2(31/34) [75.2, 97.7]	0.770 [0.657, 0.882]	0.0001
FFR _{CT} -1 cm + FFR _{CT} -2 cm	87.5(63/72) [77.9 93.3]	80.0(20/25) [58.7, 92.4]	91.5(43/47) [78.7, 97.2]	83.3(20/24) [61.8, 94.5]	89.6(43/48) [76.6, 96.1]	0.857 [0.754, 0.961]	0.0001
FFR _{CT} -2 cm + FFR _{CT} -3 cm	87.5(63/72) [77.9 93.3]	80.0(20/25) [58.7, 92.4]	91.5(43/47) [78.7, 97.2]	83.3(20/24) [61.8, 94.5]	89.6(43/48) [76.6, 96.1]	0.871 [0.774, 0.969]	0.0001
FFR _{CT} -3 cm + FFR _{CT} -lowest	86.1(62/72) [76.3 92.3]	84.0(21/25) [63.1, 94.7]	87.2(41/47) [71.6, 93.5]	77.8(21/27) [54.8,88.6]	88.9(41/45) [77.9, 88.6]	0.857 [0.756, 0.957]	0.0001
FFR _{CT} -1 cm + FFR _{CT} -2 cm + FFR _{CT} -3 cm	87.5(63/72) [77.9 93.3]	80.0(20/25) [58.7, 92.4]	91.5(43/47) [78.7, 97.2]	83.3(20/24) [61.8, 94.5]	89.6(43/48) [76.6, 96.1]	0.871 [0.774, 0.969]	0.0001
FFR _{CT} -2 cm + FFR _{CT} -3 cm + FFR _{CT} -lowest	87.5(63/72) [77.9 93.3]	80.0(20/25) [58.7, 92.4]	91.5(43/47) [78.7, 97.2]	83.3(20/24) [61.8, 94.5]	89.6(43/48) [76.6, 96.1]	0.872 [0.774, 0.970]	0.0001
CCTA + FFR _{CT} -1 cm	81.9(59/72) [79.5, 89.1]	60.0(15/25) [38.9, 78.2]	93.6(44/47) [81.4, 98.3]	83.3(15/18) [57.7, 95.6]	81.5(44/54) [68.1, 90.3]	0.785 [0.664, 0.905]	0.0001
CCTA + FFR _{CT} -2 cm	87.5(63/72) [77.9 93.3]	80.0(20/25) [58.7, 92.4]	91.5(43/47) [78.7, 97.2]	83.3(20/24) [61.8, 94.5]	89.6(43/48) [76.6, 96.1]	0.868 [0.770, 0.967]	0.0001
CCTA + FFR _{CT} -3 cm	86.1(62/72) [76.3 92.3]	84.0(21/25) [63.1, 94.7]	87.2(41/47) [71.6, 93.5]	77.8(21/27) [54.8,88.6]	88.9(41/45) [77.9, 88.6]	0.863 [0.765, 0.961]	0.0001
CCTA + FFR _{CT} -lowest	73.6(53/72) [62.4, 82.4]	88.0(22/25) [67.7, 96.8]	66.0(31/47) [50.6, 78.7]	58.0(22/38) [40.9, 73.3]	91.2(31/34) [75.2, 97.7]	0.798 [0.695, 0.902]	0.0001

PPV positive predictive value, NPV negative predictive value, CCTA coronary computed tomography angiography, DS diameter stenosis, FFR_{CT}-1 cm FFR_{CT} measured at 1 cm distal to the lower border of the target lesion, FFR_{CT}-2 cm FFR_{CT} measured at 2 cm distal to the lower border of the target lesion, FFR_{CT}-3 cm FFR_{CT} measured at 3 cm distal to the lower border of the target lesion, FFR_{CT}-lowest lowest FFR_{CT} value in the distal vessel tip. Data in parentheses are number of vessels. Data in brackets are 95% confidence interval

proximal LAD stenosis and found that it was a reliable location for measuring FFR_{CT} using invasive FFR measured 2-3 cm distal to the stenosis as reference standard. An expert panel [23] based on the finding of Cami et al. [16] advised to use the minimum FFR_{CT} values measured 1 to 2 cm distal to the stenosis as the result to judge the coronary lesion-specific ischemia. However, the measurement site proposed by Cami et al. [16] was defined as the distance from the distal end of the target stenosis to the place where FFR_{CT} declined to a lower plateau. In a similar study by Omori et al. [15], the diagnostic performance of FFR_{CT} measured at 1 to 2 cm distal to the stenosis was also found to be higher than that of FFR_{CT}-lowest (0.86 vs. 0.80, $p=0.002$) in identifying lesion-specific ischemia using invasive FFR as reference standard. In addition, Nozaki et al. [18] used a CFD-based algorithm and found that the AUC of FFR_{CT}-2 cm was higher than that of FFR_{CT}-lowest (0.80 vs. 0.68, $p=0.002$) in identifying lesion-specific ischemia and was comparable with that of FFR_{CT}-1 cm (0.80 vs. 0.79, $p=0.73$). In a recent

study by Chen et al. [24] where a machine learning-based algorithm was applied, the AUC of FFR_{CT}-2 cm was found to be comparable with that of FFR_{CT}-1 cm (0.91 vs. 0.91, $p=0.663$) and was higher than that of FFR_{CT}-3 cm (0.91 vs. 0.88, $p=0.002$) and FFR_{CT}-4 cm (0.91 vs. 0.88, $p=0.008$) in identifying lesion-specific ischemia using invasive FFR as reference standard. Based on these results, FFR_{CT} measured at 1-to-2 cm distal to the stenosis is better than FFR_{CT}-lowest in identifying lesion-specific ischemia in patients with CAD.

In our study, invasive FFR was also used as the reference standard. Our results showed that there was a good correlation ($r=0.80$, $p<0.001$) and a very mild difference (mean difference 0.0001, 95% limits of agreement: -0.1222 to 0.1220) between invasive FFR and FFR_{CT}-2 cm. Further ROC analysis showed that the diagnostic performance of FFR_{CT} measured at 2 cm distal to the target lesion (FFR_{CT}-2 cm) was higher than that measured at 1 cm distal to the target lesion (FFR_{CT}-1 cm) and that measured at the vessel terminus (FFR_{CT}-lowest)

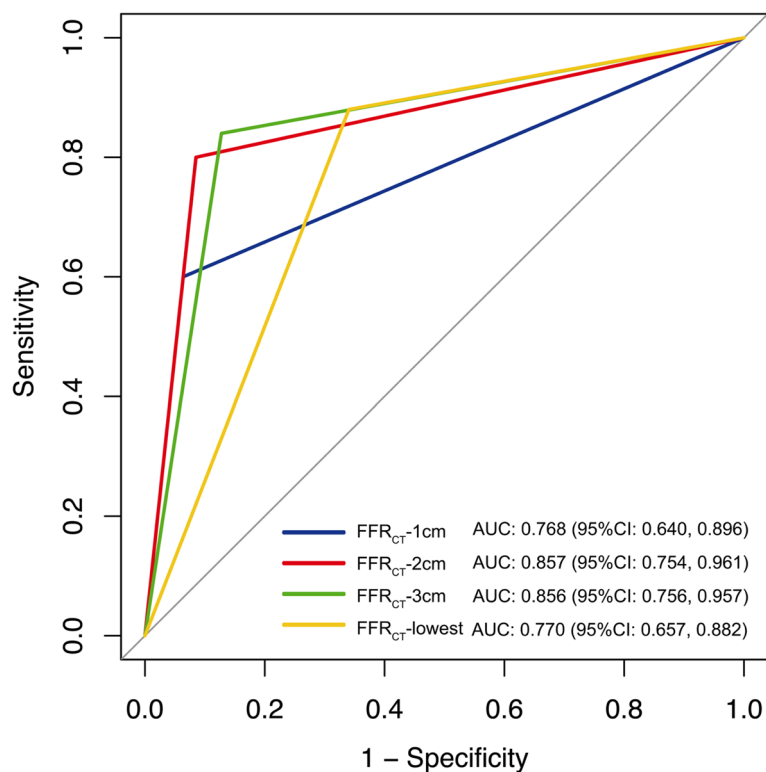


Fig. 4 Receiver operating characteristic curves of the FFR_{CT}-1 cm, FFR_{CT}-2 cm, FFR_{CT}-3 cm, FFR_{CT}-lowest per-vessel in identifying lesion ischemia with invasive FFR as the reference standard based on per-vessel analysis. The AUCs of FFR_{CT}-2 cm and FFR_{CT}-3 cm in detecting lesion-specific ischemia were significantly higher than FFR_{CT}-1 cm and the FFR_{CT}-lowest ($p < 0.05$ in each case). AUC, area under the curve

(AUC: 0.857, 0.768, 0.770, respectively), and was comparable with FFR_{CT}-3 cm (AUC: 0.856). These findings suggest that FFR_{CT} measured at 2 cm distal to the target lesion had the highest performance in identifying lesion-specific ischemia. Overall, our results are consistent with the findings of previous study [15, 16, 18, 24]. In our study, FFR_{CT} was measured at four different sites along the same artery and our results showed that FFR_{CT} measured at 2 cm distal to the target lesion are the optimal site for FFR_{CT} measurement, which is in line with previous studies [15, 16, 18, 24]. It should be noted that the measurement site of the invasive FFR and the definition of the target lesion were not totally consistent between our study and previous studies [15, 16, 18, 24]. Indeed, the invasive FFR was measured 2 to 3 cm distal to the target lesion in our study which was based on the recommendation as previously described [19], which is as same as the study by Cami et al. [16]. Nonetheless, Omori et al. [15] used invasive FFR measured 2–4 cm distal to the target lesion as the reference standard, Nozaki et al. [18] used invasive FFR measured distal to the stenosis as far as possible as the reference standard. Chen et al. [24] used invasive FFR which was measured at a minimum of 2 cm distal to the stenosis in vessel segments ≥ 2 mm as the

reference standard. As regards the target lesion, the definition of the target lesion of a serial lesion in the study by Nozaki et al. [18] was similar to our study, i.e., the most distal lesion in the vessel with 30%–90% diameter stenosis selected as the target lesion. However, Omori et al. [15] and Chen et al. [24] selected the most severe stenosis in a serial lesion as the target lesion. These differences likely result in the mild discrepancy in the diagnostic performances of FFR_{CT} measured at 1 to 2 cm distal to the target lesion. It is known that there is a gradual decrease in FFR_{CT} from proximal to distal along the vessel even without focal stenosis [16]. The lowest value of FFR_{CT} measured at 1 to 2 cm distal to the target lesion probably is not significantly different from FFR_{CT} measured 2 cm distal to the lower border of the target lesion. Thus, it is reasonable that 2 cm distal to the target lesion could be used as the exact measurement site for FFR_{CT}. Our results indicate that FFR_{CT}-2 cm is the optimal for identifying lesion-specific ischemia. This finding might impact the clinical decision-making and patient outcomes. For example, if a patient has a lesion with 30–90% vessel diameter stenosis while no lesion-specific ischemia as determined by FFR_{CT}-2 cm, this patient could avoid invasive FFR and unnecessary interventional revascularization.

Due to the presence of a gradual decrease in FFR_{CT} from proximal to distal along the vessel even without focal stenosis [16], FFR_{CT} measures at different sites along the same coronary arterial might have different clinical indication. Our study showed that FFR_{CT} -1 cm has the highest specificity (93.6%) in diagnosing lesion-specific ischemia compared with FFR_{CT} -2 cm, FFR_{CT} -3 cm and FFR_{CT} -lowest, but had the lowest sensitivity (60%); FFR_{CT} -lowest has the highest sensitivity (88%) and NPV (91.2%) in identifying lesion-specific ischemia but had the lowest specificity (66%) and PPV (58%). 18% vessels positive for FFR_{CT} -lowest were reclassified as negative when determined by FFR_{CT} -2 cm. These results indicate that FFR_{CT} -1 cm could underestimate the severity of the lesion and the FFR_{CT} -lowest could overestimate the severity of the lesion. Similarly, Kueh et al. [25] also found that FFR_{CT} -lowest overestimated the severity of the lesion when compared to FFR_{CT} measured within 20 mm of the stenotic lesion in identifying lesion-specific ischemia and false positive results of FFR_{CT} -lowest could be effectively reclassified by FFR_{CT} measured within 20 mm of the stenotic lesion. This might be associated with the gradual decrease in FFR_{CT} from proximal to distal along the vessel even without focal stenosis, which is more significant with FFR_{CT} than with invasive FFR due to pressure loss by frictional losses according to Poiseuille's equation [16]. Taken together, FFR_{CT} -1 cm and FFR_{CT} -lowest both are not optimal site for FFR_{CT} measurement and cannot be used as FFR_{CT} result in clinical decision-making.

CCTA can overestimate the severity of stenosis in CAD. It has been reported that less than a half of severe coronary artery disease diagnosed by CCTA can really result in lesion-specific ischemia [26]. This raised the concern that the widespread use of CCTA may encourage unnecessary ICA [27]. In our study, the AUC of CCTA ($DS \geq 50\%$) alone had only a moderate diagnostic performance ($AUC = 0.576$) for identifying lesion-specific ischemia, which was lower than that of FFR_{CT} -1 cm, FFR_{CT} -2 cm, FFR_{CT} -3 cm, and FFR_{CT} -lowest. When CCTA was combined with either FFR_{CT} -1 cm, FFR_{CT} -2 cm, FFR_{CT} -3 cm, or FFR_{CT} -lowest, its AUC was improved in identifying lesion-specific ischemia. These results suggest that the addition of FFR_{CT} can improve the diagnostic performance of CCTA in identifying lesion-specific ischemia and may reduce unnecessary ICA, thereby enhance its role as a gatekeeper for ICA.

Our study has some limitations. First, it is a retrospective study from a single center and the sample size was not large. It has selection bias inherent in a retrospective study. Second, patients with previous revascularization were excluded from the study. Thus, the validity of FFR_{CT} parameters in these patients needs further investigation. Third, a per-vessel analysis was performed in our study. In some patients, more than one vessel was included for

analysis. Fourth, FFR_{CT} can be calculated using a machine learning-based algorithm or a CFD-based algorithm. In our study, only CFD-based algorithm was investigated. Fifth, the long-term effect of FFR_{CT} on the adverse cardiac events was not investigated in this study. Further prospective clinical studies are warranted to validate the impact of FFR_{CT} on the clinical outcome in patients with CAD.

Conclusion

Our study demonstrates that FFR_{CT} measured at 2 cm distal to the lower border of the target lesion is the optimal measurement site in identifying lesion-specific ischemia in patients with CAD. The addition of FFR_{CT} to CCTA can improve the diagnostic performance in identifying lesion-specific ischemia. FFR_{CT} -2 cm could be used as an alternative imaging biomarker in identifying lesion-specific ischemia. The use of FFR_{CT} -2 cm can avoid unnecessary invasive FFR in a patient who has a 30%-90% diameter stenosis but negative FFR_{CT} -2 cm. This may aid in the decision-making in patients with CAD. In our study, the invasive FFR was used as a reference standard to assess the diagnostic performances of FFR_{CT} measured at different sites. Whereas the sample size was relatively small. Future multicenter prospective studies are needed to validate the clinical role of FFR_{CT} -2 cm.

Abbreviations

CAB	Gcoronary artery bypass graft surgery
CAD	Coronary artery disease
CCTA	Coronary computed tomography angiography
CFD	Computational fluid dynamics
EF	Ejection fraction
FFR	Fractional flow reserve
FFR_{CT}	Computed tomography fractional flow reserve
ICA	Invasive coronary angiography
NYHA	New York Heart Association
PCI	Percutaneous coronary intervention
ROI	Region of interest
SCCT	Society of Cardiovascular Computed Tomography

Acknowledgements

Not applicable.

Authors' contributions

ZC: conceptualization, data curation, manuscript draft, and editing. TY: data acquisition, data analysis, manuscript draft. ZY: data acquisition, data analysis. HH: data acquisition, data analysis. YL: data acquisition, data analysis. HZ: data acquisition, data analysis. MC: data acquisition, data analysis. GS: data acquisition, data analysis. JS: conceptualization, manuscript draft and editing, supervision of of the research group. All authors read and approved the final manuscript.

Funding

This work was supported by SKY Imaging Research Fund Project of China International Medical Foundation (Z-2014-07-1912-21). The funding body played no role in the design of the study and collection, analysis, interpretation of data, and in writing the manuscript.

Availability of data and materials

The datasets used and analysed during the current study available from the corresponding author on reasonable request.

Declarations

Ethics approval and consent to participate

This study was approved by the Ethics Committee of Sun Yat-Sen Memorial Hospital (No. SYSEC-KY-KS-2022-054), Sun Yat-Sen University (Guangzhou, China). All methods were carried out in accordance with relevant guidelines and regulations. The ethics committee of the Sun Yat-sen Memorial Hospital, Sun Yat-sen University that waived the need of informed consent.

Consent for publication

Not applicable.

Competing interests

The authors declare no competing interests.

Author details

¹Department of Radiology, Sun Yat-Sen Memorial Hospital, Sun Yat-Sen University, Guangzhou, China. ²Department of Cardiology, Sun Yat-Sen Memorial Hospital, Sun Yat-Sen University, Guangzhou, China.

Received: 5 January 2023 Accepted: 23 May 2023

Published online: 06 June 2023

References

- Miller JM, Rochitte CE, Dewey M, Arbab-Zadeh A, Niinuma H, Gottlieb I, Paul N, Clouse ME, Shapiro EP, Hoe J, et al. Diagnostic performance of coronary angiography by 64-row CT. *N Engl J Med*. 2008;359(22):2324–36.
- Westwood ME, Raatz HD, Misso K, Burgers L, Redekop K, Lhachimi SK, Armstrong N, Kleijnen J. Systematic review of the accuracy of dual-source cardiac CT for detection of arterial stenosis in difficult to image patient groups. *Radiology*. 2013;267(2):387–95.
- Budoff MJ, Dowe D, Jollis JG, Gitter M, Sutherland J, Halamert E, Scherer M, Bellinger R, Martin A, Benton R, et al. Diagnostic performance of 64-multidetector row coronary computed tomographic angiography for evaluation of coronary artery stenosis in individuals without known coronary artery disease: results from the prospective multicenter ACC URACY (Assessment by Coronary Computed Tomographic Angiography of Individuals Undergoing Invasive Coronary Angiography) trial. *J Am Coll Cardiol*. 2008;52(21):1724–32.
- Tonino PA, Fearon WF, De Bruyne B, Oldroyd KG, Leeser MA, Ver Lee PN, Maccarthy PA, Van't Veer M, Pijls NH. Angiographic versus functional severity of coronary artery stenoses in the FAME study fractional flow reserve versus angiography in multivessel evaluation. *J Am Coll Cardiol*. 2010;55(25):2816–21.
- Ko BS, Cameron JD, Munnur RK, Wong DTL, Fujisawa Y, Sakaguchi T, Hirohata K, Hislop-Jambrich J, Fujimoto S, Takamura K, et al. Noninvasive CT-Derived FFR Based on Structural and Fluid Analysis: A Comparison With Invasive FFR for Detection of Functionally Significant Stenosis. *JACC Cardiovasc Imaging*. 2017;10(6):663–73.
- Tonino PA, De Bruyne B, Pijls NH, Siebert U, Ikeno F, van't Veer M, Klauss V, Manoharan G, Engstrom T, Oldroyd KG, et al. Fractional flow reserve versus angiography for guiding percutaneous coronary intervention. *N Engl J Med*. 2009;360(3):213–24.
- Pijls NH, De Bruyne B, Peels K, Van Der Voort PH, Bonnier HJ, Bartunek JKJ, Kooleen JJ. Measurement of fractional flow reserve to assess the functional severity of coronary-artery stenoses. *N Engl J Med*. 1996;334(26):1703–8.
- Pijls NH, Sels JW. Functional measurement of coronary stenosis. *J Am Coll Cardiol*. 2012;59(12):1045–57.
- Tesche C, De Cecco CN, Albrecht MH, Duguay TM, Bayer RR 2nd, Litwin SE, Steinberg DH, Schoepf UJ. Coronary CT Angiography-derived Fractional Flow Reserve. *Radiology*. 2017;285(1):17–33.
- Kim HJ, Vignon-Clementel IE, Coogan JS, Figueroa CA, Jansen KE, Taylor CA. Patient-specific modeling of blood flow and pressure in human coronary arteries. *Ann Biomed Eng*. 2010;38(10):3195–209.
- Koo BK, Erglis A, Doh JH, Daniels DV, Jegere S, Kim HS, Dunning A, DeFrance T, Lansky A, Leipsic J, et al. Diagnosis of ischemia-causing coronary stenoses by noninvasive fractional flow reserve computed from coronary computed tomographic angiograms. Results from the prospective multicenter DISCOVER-FLOW (Diagnosis of Ischemia-Causing Stenoses Obtained Via Noninvasive Fractional Flow Reserve) study. *J Am Coll Cardiol*. 2011;58(19):1989–97.
- Min JK, Leipsic J, Pencina MJ, Berman DS, Koo BK, van Mieghem C, Erglis A, Lin FY, Dunning AM, Apruzzese P, et al. Diagnostic accuracy of fractional flow reserve from anatomic CT angiography. *JAMA*. 2012;308(12):1237–45.
- Norgaard BL, Leipsic J, Gaur S, Seneviratne S, Ko BS, Ito H, Jensen JM, Mauri L, De Bruyne B, Bezerra H, et al. Diagnostic performance of noninvasive fractional flow reserve derived from coronary computed tomography angiography in suspected coronary artery disease: the NXT trial (Analysis of Coronary Blood Flow Using CT Angiography: Next Steps). *J Am Coll Cardiol*. 2014;63(12):1145–55.
- Taylor CA, Fonte TA, Min JK. Computational fluid dynamics applied to cardiac computed tomography for noninvasive quantification of fractional flow reserve: scientific basis. *J Am Coll Cardiol*. 2013;61(22):2233–41.
- Omori H, Hara M, Sobue Y, Kawase Y, Mizukami T, Tanigaki T, Hirata T, Ota H, Okubo M, Hirakawa A, et al. Determination of the Optimal Measurement Point for Fractional Flow Reserve Derived From CTA Using Pressure Wire Assessment as Reference. *AJR Am J Roentgenol*. 2021;216(6):1492–9.
- Cami E, Tagami T, Raff G, Fonte TA, Renard B, Gallagher MJ, Chinnaiyan K, Bilolikar A, Fan A, Hafeez A, et al. Assessment of lesion-specific ischemia using fractional flow reserve (FFR) profiles derived from coronary computed tomography angiography (FFRCT) and invasive pressure measurements (FFRINV): Importance of the site of measurement and implications for patient referral for invasive coronary angiography and percutaneous coronary intervention. *J Cardiovasc Comput Tomogr*. 2018;12(6):480–92.
- Lotfi A, Jeremias A, Fearon WF, Feldman MD, Mehran R, Messenger JC, Grines CL, Dean LS, Kern MJ, Klein LW, et al. Expert consensus statement on the use of fractional flow reserve, intravascular ultrasound, and optical coherence tomography: a consensus statement of the Society of Cardiovascular Angiography and Interventions. *Catheter Cardiovasc Interv*. 2014;83(4):509–18.
- Nozaki YO, Fujimoto S, Aoshima C, Kamo Y, Kawaguchi YO, Takamura K, Kudo A, Takahashi D, Hiki M, Kato Y, et al. Comparison of diagnostic performance in on-site based CT-derived fractional flow reserve measurements. *Int J Cardiol Heart Vasc*. 2021;35:100815.
- Toth GG, Johnson NP, Jeremias A, Pellicano M, Vranckx P, Fearon WF, Barbato E, Kern MJ, Pijls NH, De Bruyne B. Standardization of fractional flow reserve measurements. *J Am Coll Cardiol*. 2016;68(7):742–53.
- Abbara S, Blanke P, Maroules CD, Cheezum M, Choi AD, Han BK, Marwan M, Naoum C, Norgaard BL, Rubinshtein R, et al. SCCT guidelines for the performance and acquisition of coronary computed tomographic angiography: a report of the society of Cardiovascular Computed Tomography Guidelines Committee: Endorsed by the North American Society for Cardiovascular Imaging (NASCI). *J Cardiovasc Comput Tomogr*. 2016;10(6):435–49.
- Wu FZ, Wu MT. 2014 SCCT guidelines for the interpretation and reporting of coronary CT angiography: a report of the Society of Cardiovascular Computed Tomography Guidelines Committee. *J Cardiovasc Comput Tomogr*. 2015;9(2):e3.
- DeLong ER, DeLong DM, Clarke-Pearson DL. Comparing the areas under two or more correlated receiver operating characteristic curves: a non-parametric approach. *Biometrics*. 1988;44(3):837–45.
- Norgaard BL, Fairbairn TA, Safian RD, Rabbat MG, Ko B, Jensen JM, Nieman K, Chinnaiyan KM, Sand NP, Matsuo H, et al. Coronary CT Angiography-derived Fractional Flow Reserve Testing in Patients with Stable Coronary Artery Disease: Recommendations on Interpretation and Reporting. *Radiol Cardiothorac Imaging*. 2019;1(5):e190050.
- Chen YC, Zhou F, Wang YN, Zhang JY, Yu MM, Hou Y, Xu PP, Zhang XL, Xue Y, Zheng MW, et al. Optimal Measurement Sites of Coronary-Computed Tomography Angiography-derived Fractional Flow Reserve: The Insight From China CT-FFR Study. *J Thorac Imaging*. 2022;38:194–202.

25. Kueh SH, Mooney J, Ohana M, Kim U, Blanke P, Grover R, Sellers S, Ellis J, Murphy D, Hague C, et al. Fractional flow reserve derived from coronary computed tomography angiography reclassification rate using value distal to lesion compared to lowest value. *J Cardiovasc Comput Tomogr*. 2017;11(6):462–7.
26. Meijboom WB, Van Mieghem CA, van Pelt N, Weustink A, Pugliese F, Mollet NR, Boersma E, Regar E, van Geuns RJ, de Jaegere PJ, et al. Comprehensive assessment of coronary artery stenoses: computed tomography coronary angiography versus conventional coronary angiography and correlation with fractional flow reserve in patients with stable angina. *J Am Coll Cardiol*. 2008;52(8):636–43.
27. Nissen SE. Limitations of computed tomography coronary angiography. *J Am Coll Cardiol*. 2008;52(25):2145–7.

Publisher's Note

Springer Nature remains neutral with regard to jurisdictional claims in published maps and institutional affiliations.

Ready to submit your research? Choose BMC and benefit from:

- fast, convenient online submission
- thorough peer review by experienced researchers in your field
- rapid publication on acceptance
- support for research data, including large and complex data types
- gold Open Access which fosters wider collaboration and increased citations
- maximum visibility for your research: over 100M website views per year

At BMC, research is always in progress.

Learn more biomedcentral.com/submissions

